THE JOURNAL OF PHYSICAL CHEMISTRY Letters

Letter

pubs.acs.org/JPCL

Molecular and Spin Dynamics in the Paramagnetic Endohedral Fullerene $Gd_3N@C_{80}$

B. Náfrádi,[†] Á. Antal,[‡] Á. Pásztor,[‡] L. Forró,[†] L.F. Kiss,[§] T. Fehér,[‡] É. Kováts,[§] S. Pekker,[§,∥] and A. Jánossy*[,‡]

[†]Institute of Condensed Matter Physics, Ecole Polytechnique Fédérale de Lausanne (EPFL), CH-1015 Lausanne, Switzerland

[‡]Department of Physics, Budapest University of Technology and Economics and Condensed Matter Research Group of the Hungarian Academy of Sciences, Budafoki út 8, H-1111 Budapest, Hungary

[§]Wigner Research Centre for Physics of the Hungarian Academy of Sciences, H-1525 Budapest, Hungary

[∥]Óbuda University, Doberdó út 6, H-1034 Budapest, Hungary

ABSTRACT: $Gd_3N@C_{80}$ endohedral fullerene, a starting material for a potential magnetic resonance imaging contrast agent, is investigated by high-frequency electron spin resonance (ESR) and SQUID magnetometry. The magnetic moments of the three Gd ions of the endohedral Gd_3N molecule are ferromagnetically aligned at low temperatures and are uncorrelated at high temperatures. The 4 T broad 210 and 315 GHz ESR spectra measured at 2 K are well-described by a single transition between the lowest Zeeman levels of static molecules shifted by fine structure effects. At higher temperatures there is a gradual transition to a rotating state. At ambient temperatures the rotation frequency is much larger than the fine structure broadening, and a single ESR line is observed at a gyromagnetic ratio of $g = 1.995$.

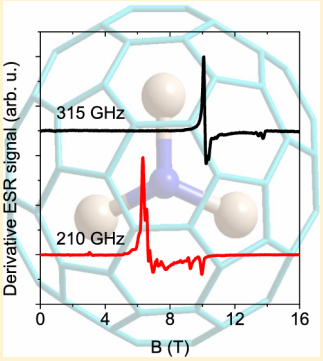

SECTION: Physical Processes in Nanomaterials and Nanostructures

Gd-filled endohedral metallofullerenes are potentially highly effective, new magnetic resonance imaging (MRI) contrast agents.[1−5] The long spin−lattice relaxation time and large magnetic moment of the spin-7/2 Gd^{3+} ions enclosed in the molecules increase the nuclear spin relaxation rate of surrounding water protons. Water-soluble functionalized endohedral magnetic metallofullerenes can enhance proton relaxivity more than Gd-containing chelates, which have been used extensively as MRI contrast agents for a long time.[6,7] In fullerenes with endohedral trimetallic nitride clusters,[8] the charge transfer from the cluster to the carbon cage stabilizes the molecule.[9] Some of the various functionalized derivatives of Gd containing endohedral trimetallic fullerenes are very promising contrast agents.[4,5]

In $Gd_3N@C_{80}$, the Gd_3N cluster forms a pyramid[9,10] filling the C_{80} cage. The Gd_3N cluster itself (outside the cage) has been experimentally and theoretically investigated;[11] it is highly magnetic with a magnetic moment of 23 μ_B mainly localized on the 4f shell of the Gd atoms. Density functional theory calculations[11] indicate that the magnetic properties of the $Gd_3N@C_{80}$ molecule are determined by the half filled 4f shell of Gd ions of the Gd_3N cluster. The endohedral fullerene, $Gd_3N@C_{80}$, has a large gap between HOMO and LUMO orbitals. In the ground-state electronic configuration the s, p, and d electrons do not contribute to the magnetism.

The key issue, how the three Gd ions are magnetically coupled within the $Gd_3N@C_{80}$ molecules, remains unclear. Calculations[12,11] predict various configurations close in energy but with very different magnetic moments. The density functional theory calculations predict that in the most stable configuration of $Gd_3N@C_{80}$ the $S = 7/2$ $4f^7$ electron spins of the three Gd^{3+} ions are noncollinear and weakly coupled antiferromagnetically into a nonmagnetic state.[12] Other calculations[11] predict a different noncollinear ground state with a magnetic moment of 14.1 μ_B. In both calculations the collinear 21 μ_B ferromagnetic state is a few millielectronvolts higher in energy.

Here we report the static magnetization $M(B,T)$ and high-frequency ESR spectra as a function of magnetic field, B, and temperature, T, of crystalline $Gd_3N@C_{80}$. A previous study of the magnetization using a special technique[13] was limited to very low temperatures. Static magnetization provides information on the absolute value of the average magnetic moment of the molecules; this is not available by ESR at high frequencies. ESR provides information on the motional state, the g factor, and some of the interactions within the molecule. It is sensitive to the anisotropies and the inhomogeneity of the molecular states within the crystal. The broadness of the ESR spectrum of $Gd_3N@C_{80}$ explains most likely why it was not observed in a previous study at 9 GHz.[10] In diluted $Gd@C_{82}$, an ESR study

Received: August 23, 2012
Accepted: October 18, 2012

   dx.doi.org/10.1021/jz301250j | J. Phys. Chem. Lett. 2012, 3, 3291−3296

showed[14] that the 7/2 spin Gd ion is coupled magnetically to a 1/2 spin cage electronic state.

We find that at 2 K the crystal is paramagnetic; the ground state of the $Gd_3N@C_{80}$ molecule is highly magnetic. The magnetic moment is about $\mu = 21\ \mu_B$ and the g factor is $g = 1.995$; that is, it is close to the $S = 21/2$ spin state of three ferromagnetically coupled Gd ions. The molecules are static, and the ESR spectrum is broadened to 4 T by the fine structure of randomly oriented molecules. At ambient temperature, the three Gd^{3+} $S = 7/2$ spins of the endohedral $Gd_3N@C_{80}$ molecule are essentially independently paramagnetic. Above $T = 150$ K, the molecules rotate rapidly. The magnetic transition between the ferromagnetically aligned and independent molecular states of the three Gd ions is complex. We suggest that the magnetic and rotational states are coupled; the ferromagnetic exchange interaction is large in static molecules and small in rotating molecules. The transition is broad; the rotation of molecules sets in gradually between 20 and 150 K.

The magnetization of $Gd_3N@C_{80}$ was measured as a function of magnetic field and temperature. The temperature dependence of $M(T)\cdot T$ at $B = 0.1$ T magnetic field is plotted in Figure 1. Zero-field-cooled and field-cooled (not shown)

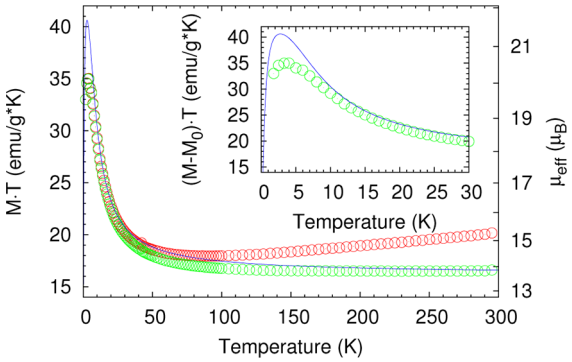

Figure 1. Temperature dependence of magnetization times temperature, $M\cdot T$ at $B = 0.1$ T plotted by red. The data corrected for a temperature-independent Van Vleck term $M_0 = 0.12$ emu/g are shown by green. The solid line is a result of the numerical calculation described in the text. Inset: zoom on the low-temperature range. Right scale: effective magnetic moment per $Gd_3N@C_{80}$ molecule. For three $S = 7/2$ and $g = 1.995$ Gd^{3+} spins, $\mu_{eff} = g(21/2\cdot 23/2)^{1/2}\ \mu_B = 21.9\ \mu_B$ when they are aligned ferromagnetically, and $\mu_{eff} = g(3\cdot 7/2\cdot 9/2)^{1/2}\ \mu_B = 13.7\ \mu_B$ when they are uncorrelated.

measurements yield identical results. The linear increase of $M(T)\cdot T$ with temperature above 100 K is attributed to a temperature-independent Van Vleck term of $M_0 = 0.12$ emu/g. The curve with corrected magnetization $(M - M_0)\cdot T$ is plotted by green symbols in Figure 1. The "effective magnetic moment", $\mu_{eff} = [(M-M_0)\cdot 3k_BT/(NB)]^{1/2}$ (where N is the concentration of $Gd_3N@C_{80}$ molecules and k_B is the Boltzmann constant), is temperature-independent at high temperatures; this is characteristic of free paramagnetic spins. The increase in μ_{eff} at low temperatures is due to a ferromagnetic coupling between the Gd spins. The inset of Figure 1 shows the low-temperature data below 30 K in more detail. μ_{eff} has a pronounced maximum at $T = 3$ K. Magnetization curves measured at fixed temperatures from 1.8 to 300 K are plotted in Figure 2 as a function of magnetic field. At $T = 300$ K, the magnetization increases linearly with field. Below 20 K, the magnetization increases nonlinearly with field, as expected for a molecule with a large magnetic moment.

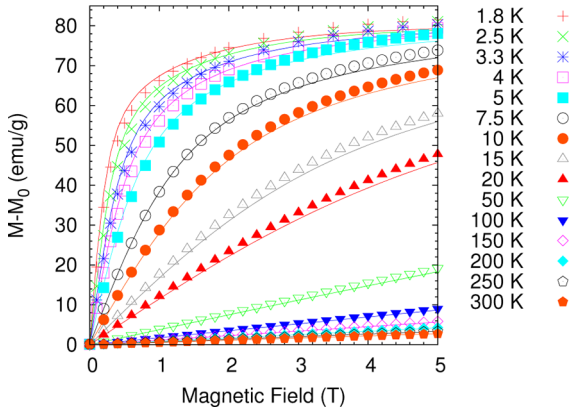

Figure 2. $M(B,T)$ as a function of the external field in the 1.8−300 K temperature range (symbols). Data were corrected for a temperature-independent ferromagnetic impurity and for a Van Vleck term, M_0. Solid lines are the result of calculations described in the text.

Figure 3 shows the 210 and 315 GHz ESR spectra recorded at $T = 2$ K by thick lines. The spectra recorded with the usual magnetic-field modulation technique are the magnetic-field derivatives of the absorption spectra. The spectra are about 4 T broad at both frequencies. The broadening is due to the anisotropy of the crystal field (or fine structure) in the randomly oriented molecules. To first order, the perturbation

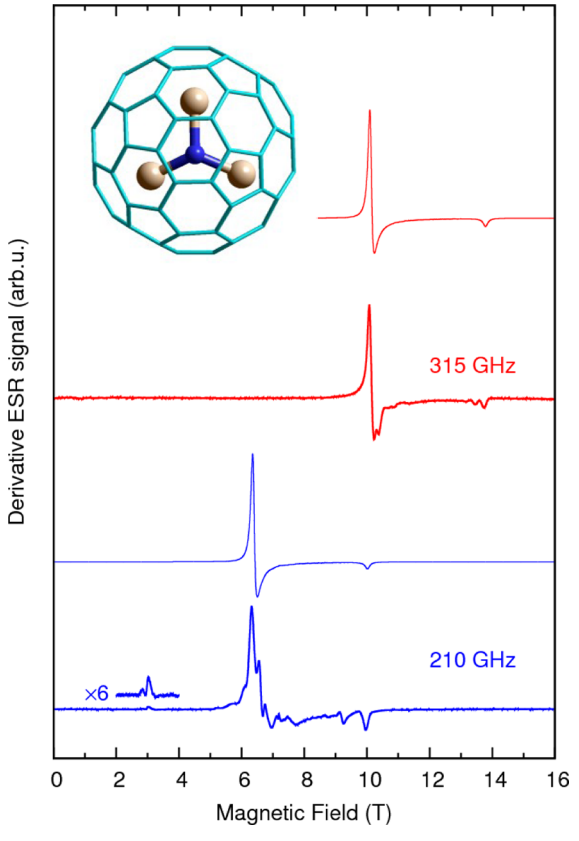

Figure 3. ESR spectra at 2 K measured at 210 and 315 GHz (thick lines). The half-field "forbidden" transition at 210 GHz is shown amplified. Thin lines are results of simulations for powder spectra as described in the text. Inset: Structure of $Gd_3N@C_{80}$ molecule projected along the axis of the Gd_3N pyramid, after ref 9. The $S = 21/2$ spin of the ferromagnetically coupled Gd ions is in a dominantly axial crystal field.

dx.doi.org/10.1021/jz301250j | J. Phys. Chem. Lett. 2012, 3, 3291−3296

of the Zeeman levels by the crystal field results in a shift independent of excitation frequency. The line shape corresponds to an approximately uniaxial crystal field as expected for the Gd_3N pyramid. Only a single transition between the lowest energy levels is excited if the Zeeman energy is much larger than the thermal energy. In an axial crystal field, the resonance frequency shift depends on the angle ϕ between the axis and B. The dominant features in the ESR spectra in Figure 3 correspond to a common powder spectrum where B is high, T is low, ϕ is random, and the shift as a function of ϕ follows a second-order Legendre polynom.[15] In the 315 GHz derivative ESR spectrum (Figure 3) the lower and higher field peaks at 10 and 13.8 T arise from static molecules with crystal field axis perpendicular and parallel to B, respectively. At 210 GHz, the crystal-field perturbation is not a small perturbation, and although the spectrum is dominated by the "allowed" lowest Zeeman transition, there are contributions from other transitions also. In particular, a weak "half field" transition appears that corresponds to the "forbidden" transition of the molecules with crystal-field axis perpendicular to the magnetic field.

The temperature evolution of the 315 GHz ESR spectrum is shown in Figure 4. The temperature dependence of the

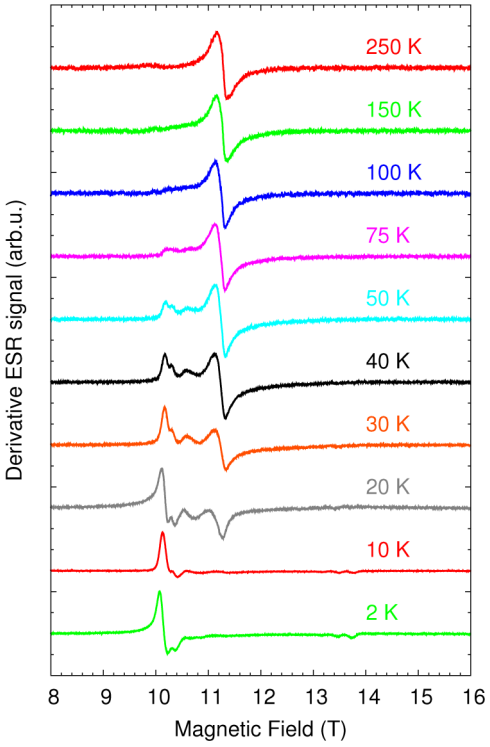

Figure 4. 315 GHz ESR spectra of $Gd_3N@C_{80}$ powder at various temperatures. Note the gradual change from a broad spectrum at 2 K to a single line at ambient temperature corresponding to the transformation between static and rotating molecules.

210 GHz spectrum is similar. By increasing the temperature from 2 to 150 K, the 4 T broad powder ESR spectrum gradually disappears and transforms into a single line. There is little change between 2 and 10 K. At 20 K a strong $\Delta H = 0.2$ T wide line appears at a g factor of $g = 1.995$. The intensity of this relatively narrow line increases with temperature, whereas its width and g factor are temperature-independent. Above 150 K only this single line is observed. The broad component fades away gradually with temperature. It has a more complicated structure at higher temperatures than at 2 K, but, judged from the low-field part of the spectrum, the width remains about 4 T. The weak and broad spectrum component is still observable at 100 K in the 315 GHz spectrum above 10 T.

We first discuss the low-temperature magnetic properties by modeling $Gd_3N@C_{80}$ molecules by the spin Hamiltonian

$$H = \sum_i H_Z(i) + H_{ZFS}(i) + \sum_{i>j} H_{ee}(i,j) = \sum_i (\mu_B g \mathbf{B}\mathbf{S}_i + D(S_{zi}^2 - \mathbf{S}_i^2/3)) + \sum_{i>j} J\mathbf{S}_i\mathbf{S}_j \quad (1)$$

where $H_Z(i)$, $H_{ZFS}(i)$, and $H_{ee}(i,j)$ are the Zeeman, the zero field splitting and the Heisenberg isotropic exchange interaction terms, respectively. $\mathbf{S}_i$ is the $S = 7/2$ spin operator for the ith Gd^{3+} ion, and S_z is its component along the uniaxial axis. The model is defined by only three parameters: the gyromagnetic factor (g factor), g, a uniaxial single ion anisotropy, D, and an isotropic exchange interaction, J, between pairs of spins of Gd_3N molecules. This simplified model provides a qualitatively correct description of the static magnetization and ESR spectrum below 20 K. It does not describe the higher temperature ESR spectra correctly because the onset of molecular motion has a profound effect.

The parameters g, D, and J characterize the individual molecules. Although they are probably non-negligible, for simplicity, we do not include magnetic dipolar and anisotropic exchange interactions between Gd^{3+} ions. The interactions between $Gd_3N@C_{80}$ molecules are neglected. The system is paramagnetic at 1.8 K, and thus intermolecular exchange J' interaction is small. This supports the prediction[11,16] that despite the significant charge transfer from the Gd_3N molecules to the cage, the spin density is localized on the 4f shell of Gd^{3+} ions. The estimated magnetic dipole interaction between $Gd_3N@C_{80}$ molecules is also small.

The energy levels E_s of the molecular spin system as a function of magnetic field were calculated by diagonalization of eq 1 using parameters determined by a fit to static magnetization and ESR spectra below 20 K. The static magnetization is calculated using the standard procedure

$$M = -\frac{N_A}{M_m}\frac{\partial F}{\partial B} \quad (2)$$

where N_A is Avogadro's number, M_m is the molar mass of $Gd_3N@C_{80}$, and F is the free energy of a single $Gd_3N@C_{80}$ molecule

$$F = -k_B T \ln Z \quad (3)$$

Z is the partition function

$$Z = \sum_s e^{-E_s/(k_B T)} \quad (4)$$

Here s indexes the 512 energy states of the system and k_B is the Boltzmann constant.

The calculated temperature- and field-dependent magnetization curves and the 2 K ESR spectra in Figures 1−3 are all obtained with the same spin Hamiltonian parameters fitted to the experimental data: the g factor $g = 1.995$, single ion anisotropy $D = 11.5$ GHz, and $J = -15$ GHz. For a consistent description of the magnetization, we assume that only 82.5% of the measured sample weight is from $Gd_3N@C_{80}$ crystals. The

dx.doi.org/10.1021/jz301250j | J. Phys. Chem. Lett. 2012, 3, 3291−3296

difference is due to a nonmagnetic substance of unknown origin, and part of it is due to measurement error of the weight. Correcting the weight, we get a consistent picture for the magnetization at high and low temperatures and as a function of field. At low temperatures, the exchange coupling between the three Gd ions results in an effective $S = 21/2$ spin. This is demonstrated by the field dependence at 1.8 K, which follows well the expectation for the three ferromagnetically coupled Gd ions. The saturation magnetization at 1.8 K and 5 T agrees with the fully polarized value. At high temperatures the small interaction between Gd spins is ineffective, and the temperature-independent value of μ_{eff} above 150 K is precisely given by three free paramagnetic $S = 7/2$ spins.

The exchange interaction is obtained from the temperature and field dependence of the static magnetization. A fit to the maximum of μ_{eff} at 3 K and 0.1 T shows (insert in Figure 1) that J is ferromagnetic and the exchange energy is small. A temperature-independent exchange of $J = -15$ GHz describes not only the 3 K maximum but also the magnetization in the full 1.8 to 300 K temperature range.

The ESR study shows, however, that this description is oversimplified. Powder ESR spectra were calculated from Figure 1 using EasySpin Matlab package.[17] The measured and simulated spectra at 2 K are compared in Figure 3 for frequencies of 210 and 315 GHz. The transition frequencies and probabilities were calculated from the spin Hamiltonian as a function of magnetic field angle and convoluted by a Lorentzian line shape with a uniform width of 0.1 T. $g = 1.995$ and $D = 11.5$ GHz were obtained by a best fit between calculated and experimental spectra at 315 GHz and 2 K. The g factor is typical for Gd^{3+} ions.[18] Between 2 and 10 K, the 315 GHz ESR spectrum is relatively simple and changes little with temperature. The high field used in the ESR fully polarizes the molecules, and only the lowest energy transition between the $S_z = 21/2$ and 19/2 Zeeman levels of the $S = 21/2$ spin state is observed. The 210 GHz spectrum is somewhat more complicated; some smaller intensity lines appear, which are characteristic of transitions between energy levels close to the ground state. The calculation reproduces the position of the "forbidden" transition at half field but not the intensity. Some details, in particular the doubling of the high field line, are not reproduced by the calculation. We attribute the double peak to two slightly different molecular configurations with nearly the same energy and anisotropies of $D = 11$ and 11.5 GHz. Small variations in the position and structure of the pyramidal cluster within the distorted I_h symmetry cage can explain the double peak. Such variations were observed[9] in the X-ray structure of crystalline $Gd_3N@C_{80}\cdot(NiC_{36}H_{44}N_4)\cdot 1.5(C_6H_6)$.

The collinear ferromagnetic ground state of $Gd_3N@C_{80}$ found in the present work is rather different from the complex ground state suggested for other $Re_3N@C_{80}$ (Re = Ho,Tb) materials.[19,20] In these compounds, ligand fields are strong within the cluster and a temperature- and field-independent noncollinear 120° alignment of the rare earth spins was observed. Recent density functional calculations predicted a noncollinear 120° ground state[12] also for $Gd_3N@C_{80}$, but this is contradicted by the present experiments.

Above 20 K the temperature evolution of the ESR spectra, shown for 315 GHz in Figure 4, does not confirm the simple picture based on a temperature independent energy structure of static molecules. The calculated ESR spectra at 50 (Figure 5d) and 150 K (not shown), using the same spin Hamiltonian parameters as for 2 K, differ qualitatively from the observed

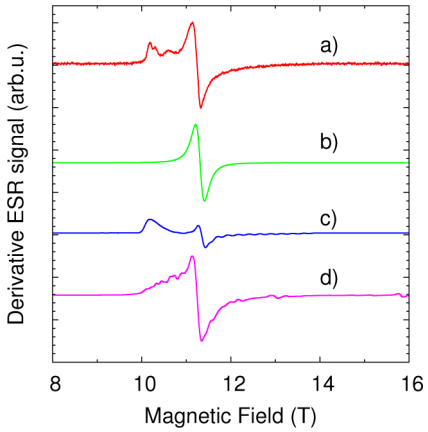

Figure 5. Simulations of the ESR spectrum at 50 K. (a) Measured and (b–d) calculated spectra. (b) Motionally narrowed line of fast rotating molecules. (c) Fine structure broadened line of three static ferromagnetically aligned Gd^{3+} ions. (d) Spectrum of Gd^{3+} ions coupled by a weak, temperature-independent coupling of $J = -15$ GHz. The main features of curve (a) are reproduced by a superposition of curves (b) and (c) but are not reproduced by curve (d).

spectra. First, although a large intensity peak centered around $g = 1.995$ is correctly predicted, the calculated central peak has slowly decaying wings on both sides. These wings, due to unresolved allowed Zeeman transitions of static molecules with randomly oriented crystal fields, are predicted to persist to high temperatures. However, the intensity around the center of the observed spectrum decreases faster than predicted by increasing temperature. The ESR at 150 K has a Lorentzian shape. Second, contrary to the measured spectra, the calculation predicts negligible intensity at the end of the spectrum at ~10.2 T. However, the intense peak due to the 21/2→19/2 transition at 2 K is clearly present in the observed spectrum at 50 K and is still observable at 100 K; it disappears only at 150 K.

The large intensity at the transition between the lowest Zeeman levels at 10.2 T means that in a large fraction of molecules the three Gd spins are in the ferromagnetic $S = 21/2$ state. This contradicts the assumptions made in the calculation of the static magnetization (Figures 1 and 2). In the calculation based on a temperature-independent $J = -15$ GHz, the Gd spins are effectively uncoupled at 50 K; the fraction of molecules in high spin states is negligible.

The most important features of the ESR spectra are reproduced by assuming that due to disorder the material is inhomogeneous and there is a very broad transition from a phase with static molecules to a phase with rotating molecules. For the sake of demonstration of the qualitative behavior, we assume that at intermediate temperatures, between 20 and 100 K, there are two types of molecules. Molecules in the ground state are described by the spin Hamiltonian with $D = 11.5$ GHz and $g = 1.995$ and a ferromagnetic coupling that is much stronger than $J = -15$ GHz used previously to describe the magnetization assuming a homogeneous sample. Therefore, molecules in the ground state may remain in the $S = 21/2$ magnetic state up to higher temperatures. The larger J does not change the 2 K spectrum. Molecules in excited states rotate and are assumed to have a much smaller J. In the excited molecules, the three $S = 7/2$ Gd ions are uncoupled at all temperatures. The rotation around random axes motionally narrows the ESR

dx.doi.org/10.1021/jz301250j | J. Phys. Chem. Lett. 2012, 3, 3291–3296

of the molecules, explaining the lack of wings around the central line. The single Lorentzian line of the 150 K spectrum arises from rapidly rotating molecules. Motional averaging of the broad spectrum into a narrow line sets in for rotation frequencies of 10^9 to 10^{10} Hz depending on D and J in the rotating state. The narrow features in the static spectrum show that "static" molecules rotate with a frequency less than 5×10^8 Hz. Because the static spectrum persists to 100 K, it is safe to assume that at 2 K molecules are static in the usual sense of the term. The surprise is not that molecules are static but rather that some are rotating at temperatures as low as 20 K. In $Sc_3N@C_{80}$, the molecular rotation sets in at much higher temperatures.[21]

The ESR spectra expected from the model at 50 K are shown in Figure 5c. The calculated spectrum of the $S = 21/2$ static molecules at 50 K extends to the same magnetic field as that at 2 K because the lowest Zeeman energies are still larger than the temperature (Figure 5c). The ESR of the rotating molecules is simulated in Figure 5b by a single Lorentzian line. The sum of the spectra of static and rotating molecules clearly captures the main features. Although the model explains qualitatively the static magnetization and the ESR spectra in the full temperature range, it is certainly oversimplified. There are probably several molecular configurations with various magnetic states that play a role, not just a static and a randomly rotating state, as assumed here.[12,22] The assumption of rotation for the low magnetization states is plausible, but a similar spectrum would arise from a static molecule, where the anisotropy is small for some other reason. It is also possible that in the excited state spin relaxation wipes out all transitions except the $1/2 \rightarrow -1/2$ transition, which in first order is independent of the anisotropy.

Recent NMR studies of $Sc_3N@C_{80}$[8,21] show that above an onset temperature of 130 K the molecules rotate within the crystal. The endohedral Sc_3N cluster is not rigidly fixed to the cage but rotates independently. From the present ESR study, we cannot distinguish between independent rotations of the Gd_3N cluster and the cage or other types of motion.

In conclusion, the results open a new avenue for the investigation of the magnetism of trimetallic nitride fullerene MRI contrast agents. The magnetic properties in crystalline $Gd_3N@C_{80}$ are related to the 4f shell of Gd atoms and depend mainly on the coupling between Gd ions within the cluster. The charge transferred from the Gd_3N cluster to the cage does not seem to play a role in the magnetism. This is probably also the case for functionalized trimetallic nitride molecules. $Gd@C_{82}$ is different; here the reactive magnetic cage tends to form dimers.[14] Further work on diluted functionalized systems is called for.

The interaction between molecules is small. The paramagnetism at temperatures as low as 1.8 K is the best reason to believe that the ESR reflects the properties of the individual molecules. Indeed, at 2 K, the static magnetic susceptibility and the high-frequency ESR spectrum are well-described by a simple Hamiltonian neglecting intermolecular interactions. In the ground state, the $S = 7/2$ spins of the Gd_3N cluster are ferromagnetically aligned, and the magnetic moment is close to 21 μ_B. The broad ESR spectrum is well-simulated by $S = 21/2$ spins with $g = 1.995$ in randomly oriented crystallites with an axial crystal field of $D = 11.5$ GHz. At high temperatures above 150 K, the Gd $S = 7/2$ spins are uncoupled; the susceptibility is given by the paramagnetism of the three 7 μ_B Gd ions and a small Van Vleck contribution. The plausible interpretation of the relatively narrow ESR at $g = 1.995$ is that molecules rotate rapidly around randomly varying axes. The transition from the low-temperature high-spin molecular state to the high-temperature state of uncoupled Gd spins is not simple. Although the magnetization is apparently well-described by a simple spin Hamiltonian with a set of temperature independent parameters, this description is not confirmed by the ESR spectra. In particular, the observation of static, randomly oriented molecules of $S = 21/2$ up to 100 K contradicts the small temperature-independent exchange integral, J, required to describe the magnetization. The ESR shows that the material is inhomogeneous in the broad temperature range of 20 to 100 K, where the transition from a static to a rotational state takes place.

EXPERIMENTAL METHODS

$Gd_3N@C_{80}$ fullerene powder was supplied by SES Research. We dissolved the sample in toluene and filtered it to remove potential insoluble materials and checked the quality with high-performance liquid chromatography (HPLC). The HPLC chromatogram of $Gd_3N@C_{80}$ was taken on an analytical (4.6 mm × 250 mm) Cosmosil "Buckyprep" column in toluene eluent with 330 nm UV detection. Besides $Gd_3N@C_{80}$, no other fullerene or contaminants were detected. After a multistep recrystallization from toluene, the sample was dried in dynamic vacuum for 12 h. The synthesized polycrystalline sample has an fcc structure according to powder X-ray diffraction measurement. Further details will be published elsewhere.[23] Static magnetization as a function of field and temperature and ESR at two frequencies as a function of temperature was measured on the amorphous and recrystallized samples with similar results. In particular, the magnetic field and temperature dependence of the static magnetization were very similar if the masses of $Gd_3N@C_{80}$ were corrected to take into account the presence of a diamagnetic material of unknown origin. As detailed in the discussion, we correct the measured mass of 3.649 mg of the fcc powder by a factor of 0.825 and use 3.010 mg throughout the paper. All data presented in this letter are on this recrystallized fcc powder. The static magnetization was measured with a Quantum Design MPMS-5S SQUID magnetometer between 1.8 and 300 K in magnetic fields up to 5 T. The data were corrected for a small ferromagnetic impurity with a temperature-independent saturation moment of $M_{FM} = 0.094$ emu/g and for the magnetization of the sample holder measured independently. ESR on the same powder was measured with a home-built quasi-optical spectrometer at 210 and 315 GHz in magnetic fields between 0 and 16 T[24,25] at temperatures between 2 and 250 K.

AUTHOR INFORMATION

Corresponding Author

*E-mail: atj@szfki.hu.

Notes

The authors declare no competing financial interest.

ACKNOWLEDGMENTS

We acknowledge the support of the Hungarian National Research Fund OTKA NN76727, CNK80991, T72954, K107228, the New Hungary Development Plan TÁMOP-4.2.1/B-09/1/KMR-2010-0002, and the Swiss NSF and its NCCR MaNEP. É.K. acknowledges support of the Bolyai János Scholarship of the Hungarian Academy of Sciences.

REFERENCES

(1) Mikawa, M.; Kato, H.; Okumura, M.; Narazaki, M.; Kanazawa, Y.; Miwa, N.; Shinohara, H. Paramagnetic Water-Soluble Metallofullerenes Having the Highest Relaxivity for MRI Contrast Agents. *Bioconjugate Chem.* **2001**, *12*, 510−514.

(2) Sitharaman, B.; Bolskar, R. D.; Rusakova, I.; Wilson, L. J. Gd@$C_{60}[C(COOH)_2]_{10}$ and Gd@$C_{60}(OH)_x$: Nanoscale Aggregation Studies of Two Metallofullerene MRI Contrast Agents in Aqueous Solution. *Nano Lett.* **2004**, *4*, 2373−2378.

(3) Shu, C. Y.; Zhang, E. Y.; Xiang, J. F.; Zhu, C. F.; Wang, C. R.; Pei, X. L.; Han, H. B. Aggregation Studies of the Water-Soluble Gadofullerene Magnetic Resonance Imaging Contrast Agent: $[Gd@C_{82}O_6(OH)_{16}(NHCH_2CH_2COOH)_8]_x$. *J. Phys. Chem. B* **2006**, *110*, 15597−15601.

(4) Zhang, J. F.; et al. High Relaxivity Trimetallic Nitride Gd_3N Metallofullerene MRI Contrast Agents with Optimized Functionality. *Bioconjugate Chem.* **2010**, *21*, 610−615.

(5) Braun, K.; Dunsch, L.; Pipkorn, R.; Bock, M.; Baeuerle, T.; Yang, S.; Waldeck, W.; Wiessler, M. Gain of a 500-Fold Sensitivity on an Intravital MR Contrast Agent Based on an Endohedral Gadolinium-Cluster-Fullerene-Conjugate: A New Chance in Cancer Diagnostics. *Int. J. Med. Sci.* **2010**, *7*, 136−146.

(6) Lauffer, R. B. Paramagnetic Metal-Complexes as Water Proton Relaxation Agents For NMR Imaging - Theory and Design. *Chem. Rev.* **1987**, *87*, 901−927.

(7) Caravan, P.; Ellison, J. J.; McMurry, T. J.; Lauffer, R. B. Gadolinium(III) Chelates as MRI Contrast Agents: Structure, Dynamics, And Applications. *Chem. Rev.* **1999**, *99*, 2293−2352.

(8) Stevenson, S.; et al. Small-Bandgap Endohedral Metallofullerenes in High Yield and Purity. *Nature* **1999**, *401*, 55−57.

(9) Stevenson, S.; Phillips, J. P.; Reid, J. E.; Olmstead, M. M.; Rath, S. P.; Balch, A. L. Pyramidalization of Gd_3N Inside a C_{80} Cage. the Synthesis and Structure of $Gd_3N@C_{80}$. *Chem. Commun.* **2004**, 2814−2815.

(10) Krause, M.; Dunsch, L. Gadolinium Nitride Gd_3N in Carbon Cages: The Influence of Cluster Size and Bond Strength. *Angew. Chem., Int. Ed.* **2005**, *44*, 1557−1560.

(11) Qian, M. C.; Ong, S. V.; Khanna, S. N.; Knickelbein, M. B. Magnetic Endohedral Metallofullerenes with Floppy Interiors. *Phys. Rev. B* **2007**, *75*, 104424.

(12) Lu, J.; Sabirianov, R. F.; Mei, W. N.; Gao, Y.; Duan, C. G.; Zeng, X. C. Structural and Magnetic Properties of $Gd_3N@C_{80}$. *J. Phys. Chem. B* **2006**, *110*, 23637−23640.

(13) Chen, L.; Carpenter, E. E.; Hellberg, C. S.; Dorn, H. C.; Shultz, M.; Wernsdorfer, W.; Chiorescu, I. Spin transition in $Gd_3N@C_{80}$, Detected by Low-Temperature on-Chip SQUID Technique RID A-2797−2010. *J. Appl. Phys.* **2011**, *109*, 07B101.

(14) Furukawa, K.; Okubo, S.; Kato, H.; Shinohara, H.; Kato, T. High-Field/High-Frequency ESR Study of Gd@C_{82}-I. *J. Phys. Chem. A* **2003**, *107*, 10933−10937.

(15) Slichter, C. P. *Principles of Magnetic Resonance*, 3rd ed.; Springer-Verlag: New York, 1992; p 615.

(16) Popov, A. A.; Dunsch, L. Electrochemistry In Cavea: Endohedral Redox Reactions of Encaged Species in Fullerenes RID A-9937−2011. *J. Phys. Chem. Lett.* **2011**, *2*, 786−794.

(17) Stoll, S.; Schweiger, A. Easyspin, A Comprehensive Software Package for Spectral Simulation and Analysis in EPR. *J. Magn. Reson.* **2006**, *178*, 42−55.

(18) Abragam, A.; Bleaney, B. *Electron Paramagnetic Resonance of Transition Ions*; Clarendon Press: Oxford, U.K., 1970.

(19) Wolf, M.; Muller, K. H.; Eckert, D.; Skourski, Y.; Georgi, P.; Marczak, R.; Krause, M.; Dunsch, L. Magnetic Moments in $Ho_3N@C_{80}$ and $Tb_3N@C_{80}$. *J. Magn. Magn. Mater.* **2005**, *290*, 290−293.

(20) Wolf, M.; Muller, K. H.; Skourski, Y.; Eckert, D.; Georgi, P.; Krause, M.; Dunsch, L. Magnetic Moments of the Endohedral Cluster Fullerenes $Ho_3N@C_{80}$ and $Tb_3N@C_{80}$: The Role of Ligand Fields. *Angew. Chem., Int. Ed.* **2005**, *44*, 3306−3309.

(21) Gorny, K. R.; Pennington, C. H.; Martindale, J. A.; Phillips, J. P.; Stevenson, S.; Heinmaa, I.; Stern, R. Molecular Orientational Dynamics of the Endohedral Fullerene $Sc_3N@C_{80}$ As Probed by ^{13}C and ^{45}Sc NMR, 2006. arXiv: http://arxiv.org/abs/cond-mat/0604365.

(22) Qian, M. C.; Khanna, S. N. An Ab Initio Investigation on the Endohedral Metallofullerene Gd_3N-C_{80}. *J. Appl. Phys.* **2007**, *101*, 09E105.

(23) Kovats, E.; Bortel, G.; Pekker, S. Unpublished, 2012.

(24) Náfrádi, B.; Gaál, R.; Sienkiewicz, A.; Fehér, T.; Forró, L. Continuous-Wave Far-Infrared ESR Spectrometer for High-Pressure Measurements. *J. Magn. Reson.* **2008**, *195*, 206.

(25) Náfrádi, B.; Gaál, R.; Fehér, T.; Forró, L. Microwave Frequency Modulation in Continuous-Wave Far-Infrared ESR Utilizing a Quasioptical Reflection Bridge. *J. Magn. Reson.* **2008**, *192*, 265.